Journal of
Marine Science and Engineering

MDPI

Article

A Prototype Design and Sea Trials of an 11,000 m Autonomous and Remotely-Operated Vehicle Dream Chaser

Zhe Jiang [1], Bin Lu [1], Biao Wang [1], Weicheng Cui [2,*], Jinfei Zhang [1], Ruilong Luo [1], Gaosheng Luo [1], Shun Zhang [1] and Zhongjun Mao [1]

1 Shanghai Engineering Research Center of Hadal Science and Technology, College of Engineering Science and Technology, Shanghai Ocean University, Shanghai 201306, China; zjiang@shou.edu.cn (Z.J.); m190601135@st.shou.edu.cn (B.L.); b-wang@shou.edu.cn (B.W.); jf-zhang@shou.edu.cn (J.Z.); rlluo@shou.edu.cn (R.L.); gsluo@shou.edu.cn (G.L.); szhang@autosubsea.com (S.Z.); zjmao@shou.edu.cn (Z.M.)

2 Key Laboratory of Coastal Environment and Resources of Zhejiang Province (KLaCER), School of Engineering, Westlake University, Hangzhou 310030, China

* Correspondence: cuiweicheng@westlake.edu.cn

Abstract: To better study the biology and ecology of hadal trenches for marine scientists, the Hadal Science and Technology Research Center (HAST) of Shanghai Ocean University proposed to construct a movable laboratory that includes a mothership, several full-ocean-depth (FOD) submersibles, and FOD landers to obtain samples in the hadal trenches. Among these vehicles, the project of an FOD autonomous and remotely-operated vehicle (ARV) named "Dream Chaser" was started in July 2018. The ARV could work in both remotely-operated and autonomous-operated modes, and serves large-range underwater observation, on-site sampling, surveying, mapping, etc. This paper proposed a novel three-body design of the FOD ARV. A detailed illustration of the whole system design method is provided. Numerical simulations and experimental tests for various sub-systems and disciplines have been conducted, such as resistance analysis using the computational fluid mechanics method and structural strength analysis for FOD hydrostatic pressure using the finite element method and pressure chamber tests. In addition, components tests and the entire system tests have been performed on land, underwater, and in the pressure chamber in the laboratory of HAST, and the results are discussed. Extensive experiments of two critical components, i.e., the thrusters and ballast-abandoning system, have been conducted and further analyzed in this paper. Finally, the procedures and results of lake trials, South China Sea trials and the first phase of Mariana Trench sea trials of the ARV in 2020 are also introduced. This paper provides a design method for the novel three-body FOD ARV. More importantly, the lessons learned from the FOD pressure test, lake tests, and sea trials, no matter the success or failure, will guide future endeavors and the application of ARV Dream Chaser and underwater vehicles of this kind.

Keywords: full-ocean-depth (FOD) submersible; autonomous and remotely-operated vehicle (ARV); pressure chamber tests; lake tests; sea trials

check for updates

Citation: Jiang, Z.; Lu, B.; Wang, B.; Cui, W.; Zhang, J.; Luo, R.; Luo, G.; Zhang, S.; Mao, Z. A Prototype Design and Sea Trials of an 11,000 m Autonomous and Remotely-Operated Vehicle Dream Chaser. *J. Mar. Sci. Eng.* **2022**, *10*, 812. https://doi.org/10.3390/jmse10060812

Academic Editor: Cristiano Fragassa

Received: 4 May 2022
Accepted: 11 June 2022
Published: 14 June 2022

1. Introduction

The deep ocean zones with a water depth larger than 6500 m are defined as hadal zones [1,2]. In recent years, hadal science, which relates to scientific research in hadal zones, has become the frontier of marine sciences [3,4]. Scientific activities in hadal zones rely heavily on developing full ocean depth (FOD) vehicles, including human occupied vehicles (HOVs), unmanned submersibles, landers, etc. In the last five years, remarkable progress has been made in marine biology, geography, geochemistry, and marine environmental science related to hadal zones (e.g., [5,6]). These progress and scientific discoveries could be in large part contributed to by samples obtained by all kinds of underwater vehicles that can operate at full ocean depth.

The earliest exploration of FOD vehicles dates back to 1960, when the human-piloted Bathyscaph Trieste, developed by Auguste Piccard, made one successful dive to the Challenger Deep [7]. To date, only four FOD HOVs have ever reached the deepest place on Earth—Challenger Deep of the Mariana Trench at 11°22′ N, 142°25′ E in the Western Pacific Ocean near the island of Guam [8]. Besides Trieste, on 26 March 2012, movie director James Cameron took his privately built one-person submersible 10,898 m down to the deepest point on Earth for the second time for human beings [9]. Recently, in June of 2020, Victor Vescovo conducted multiple dives to the bottom of the Challenger Deep using the crewed deep submergence vehicle (DSV), Limiting Factor, achieving the deepest observed seafloor depth of 10,935 m (±6 m at 95% confidence interval) below mean sea level [10]. More recently, in 2020, China successfully conducted a sea trial for its full-ocean depth manned submersible Fendouzhe. Thirteen dives were completed at the Challenger Deep of the southern Mariana Trench, eight exceeding 10,000 m, with a maximum dive depth of 10,909 m [11].

On the one hand, HOVs allow scientists to observe on-site and make instant decisions on what kind of samples to take, which is irreplaceable compared with unmanned submersibles. On the other hand, unmanned submersibles have advantages in terms of longer observation range, more flexibility, fewer costs, and most importantly, no risk of loss of human beings. Therefore, the desire to develop FOD unmanned submersibles is even stronger. There are mainly three types of unmanned submersibles, i.e., remotely-operated vehicle (ROV), autonomous underwater vehicle (ARV), and autonomous and remotely-operated vehicle (ARV) [12].

In 1995, the ROV Kaiko, developed by the Japan Agency for Marine-Earth Science and Technology (JAMSTEC), made the first of 20 successful dives to the Challenger Deep [13], but the vehicle was lost in 2003 [14]. In 2008, another full ocean depth (FOD) ROV built by JAMESTEC, ABISMO, successfully took sediments and water samples from the Mariana Trench [15], but ABISMO was also lost in 2016. In 2009, the ARV Nereus developed by the Woods Hole Oceanographic Institution reached the Challenger Deep twice [12]. Unfortunately, Nereus was also lost during its dive to the Kermadec Trench in 2014 [16]. In 2016, the ARV HAIDOU, developed by Shenyang Institute of Automation, Chinese Academy of Sciences, also arrived at the Challenger Deep [17]. However, HAIDOU was also lost in the next year.

Due to the problems of structural integrity and sealing issues to bear 11,000 m hydrostatic pressure, remote control technology, underwater power supply technology, limited emergency recovery measures, etc., many technical challenges need to be breakthrough in the development of FOD unmanned submersibles. Achievements have been obtained to return the unmanned submersibles to the Challenger Deep, especially in the recent three years. In May 2020, Russia's AUV Vityaz-D arrived at the Challenger Deep with a water depth of 10,028 m, first as an AUV [18]. Then, a newly built ARV HAIDOU 1 of China returned to the Challenger Deep again in June 2020 [19].

Besides the above vehicles, the hadal science and technology research center (HAST) of Shanghai Ocean University has decided to construct a movable laboratory which includes a mothership, three FOD landers, a FOD hybrid autonomous and remotely-operated vehicle (ARV), and an FOD HOV [20]. In such circumstances, an FOD ARV Dream Chaser was proposed for development in July of 2018, dedicated to filling the FOD unmanned submersibles gap at the time.

The ARV was designed to be capable of working in full ocean depth, and its main missions were set as follows: (1) To carry out underwater observation through videos, still cameras, and imaging sonar. (2) To carry out marine environment characterization by measuring the temperature, salinity, depth, turbidity, and pH values. (3) To deploy and recover light-duty sampling tools through the electric manipulator. Based on the above requirements, the project for this ARV Dream Chaser was carried out in July of 2018, and components tests in the pressure chamber, the assembly and on-land tests, and open water tank tests were completed at the end of 2019. Despite the sudden breakout of the coronavirus pandemic in China in 2020, the lake tests and sea trials in the South China Sea and Mariana Trench still strived to finish in 2020.

To achieve the above missions, this paper proposes a novel three-body design for the FOD ARV Dream Chaser, which is designed to have better stability and a direct path for maintenance. Since its global configuration differs from conventional unmanned submersibles using monohulls, a detailed illustration of the whole system design method is provided. Numerical simulations for various systems and disciplines have been conducted. In addition, different from the designs of ROVs or AUVs, the procedures, communication, and control methods for various working modes for Dream Chaser are also studied. To validate the design of the ARV, components tests and entire system tests have been conducted for on-land, underwater, and pressure tests. Finally, the results of a series of the lake trials, South China Sea trials, and Mariana trench sea trials of the ARV are given.

The design method and numerical analysis for the whole system and each major subsystem are presented in Section 2. The laboratory test of key components and results analysis are introduced in Section 3. Then, the lake tests and two phases of sea trials of the ARV are illustrated in Sections 4 and 5, respectively. Finally, Section 6 provides the concluding remarks.

2. Mission and Design of the ARV

2.1. Overview of Mission and Performance Requirements for Dream Chaser

2.1.1. Operating Environment Conditions

(1) Maximum operating water depth: 11,000 m;
(2) Sea conditions: sea state 3 for launching and sea state 4 for recovery;
(3) Bottom current speed less than 1.0 knot;
(4) The support ship has a dynamic positioning system, an unrestricted navigation area, and an armored electro-optic cable.

2.1.2. Performance Requirements

The basic functions of the ARV Dream Chaser are listed as follows.

(1) Underwater automatic heading, depth control, and altitude navigation control;
(2) Measurement and data recording of seawater temperature, salinity, depth, etc.;
(3) Underwater environmental data monitoring and recording;
(4) Accurate mapping of underwater terrain;
(5) Underwater virtual reality imaging;
(6) Sampling capability: macrobiological trapping, seawater, sediments;
(7) Large-scale surveying and mapping of underwater terrain;
(8) Equipped with other instruments in potential needs.

2.2. System Overview

2.2.1. System Configurations

Figure 1 shows the whole system of the 11,000 m unmanned submersible Dream Chaser. It consists of four parts: a submersible (i.e., the ARV), a simplified tether management system (TMS), a ship-based integrated control system, and a launch and recovery system (LARS).

The components of an ARV are very much like the HOV except for the human-related systems, such as manned cabin, life support system, etc. The ARV Dream Chaser consists of nine subsystems: buoyancy system, structural system, propulsion system, observation and communication system, positioning and navigation system, power distribution system, control system, descent, ascent weight and emergency-ascent system, and tooling system. The detailed design of each subsystem will be described in Section 2.3.

The TMS, ship-based integrated control system, and LARS are auxiliary systems for operation on the sea. Compared with TMS used in work-class ROVs, the TMS here is a simplified one that only serves as a fiber optic communications relay bridge since the ARV cannot be launched to the bottom of 11,000 m water depth directly through the electro-optic cable. The ship-based integrated control system is the operator's center of monitor and operation. The LARS is used to launch and recover the ARV and TMS.

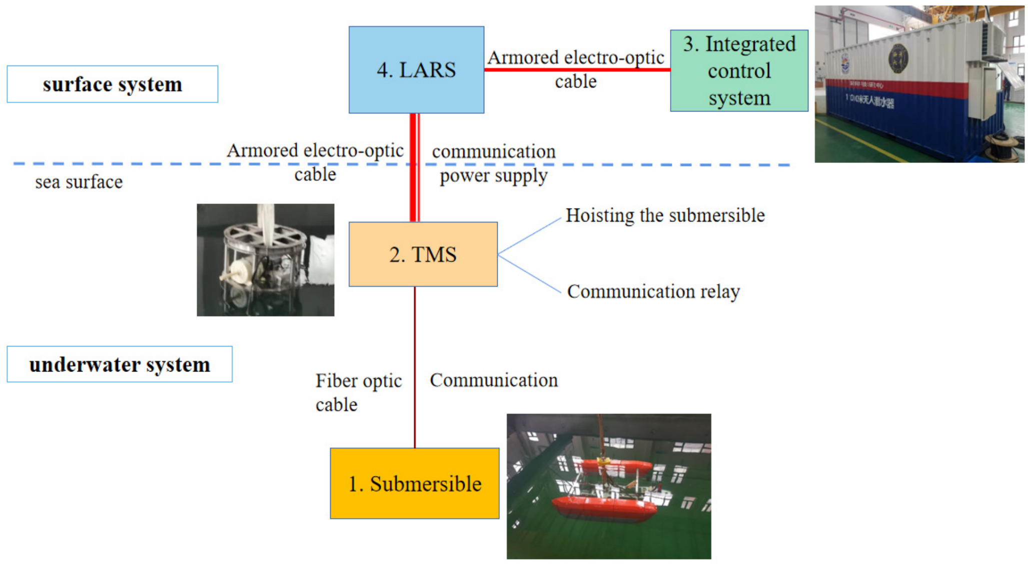

Figure 1. The whole system illustration of the ARV Dream Chaser.

2.2.2. Operation Modes

Operation modes represent the working method of an underwater vehicle. For an ARV, there are normally two operational modes, i.e., the remotely-operated mode and the autonomous-operated mode. Besides, several emergency operation strategies are designed for the sake of safety.

Remotely-Operated Mode:

The remotely-operated mode is mostly used for this ARV. A standard operating procedure of remotely-operated mode is described as follows.

(1) Deck preparation. When all of the preparation is ready, the system starts to be powered. Make the TMS and ARV engaged through the hook, and get ready for launch.
(2) Launching. Hoist the ARV and TMS together, and launch them until about 5 m below the sea surface by the LARS. Perform the system inspection.
(3) Continue to lay the TMS and the vehicle to a certain water depth below water where the current is very low. Keep the lowering speed at about 40–50 m/min. When reaching the designated depth, check the system again.
(4) The vehicle is unhooked from the TMS and starts unpowered descent by its negative buoyancy. The descending speed is dependent on the negative buoyancy weight, descending resistance, etc. The fiber optic cable installed on the vehicle and the TMS will be automatically and passively extracted.
(5) When the ARV approaches near the seafloor, abandon the descent ballast. In this design, the maximum acoustic detection range of the altimeter is 150.0 m above the sea bottom. After dumping the descent ballast, the submersible's speed slows down rapidly, and the vehicle will achieve a near-equilibrium state with a positive buoyancy of about 5–10 kgf. Use the vertical thruster to move the vehicle about 1.5 m above the sea bottom and keep the ARV in auto-depth mode.
(6) Near bottom operation to finish designated tasks. The vehicle is controlled remotely by operators on the ship. The energy of all the actions is from its self-installed battery rather than from the power on the ship. The relationship of each system during the operation period is shown in Figure 2.
(7) After the tasks are completed, abandon the ascent ballast, and the vehicle starts to float. Meanwhile, recover the TMS through the LARS. Since there is quite a long

distance between the TMS and the ARV, the TMS will return to the sea surface first and will be recovered back to the ship deck easily using the LARS.

(8) As the ARV is ascending, the operators monitor its position through USBL. When the vehicle returns to the sea surface, it will be expected to be located with the surface positioning equipment. Once the vehicle is found, the support ship will help move near the submersible and recover it using another hook or crane and wire rope other than the hook fixed with the TMS.

(9) Maintenance and be ready for the next diving.

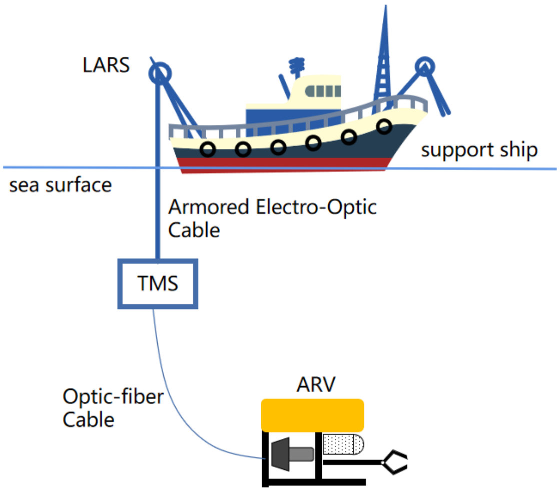

Figure 2. The position relationship of each system during the operation period.

Autonomous-Operated Mode:

In the autonomous-operated mode, the ARV will descend by itself from the sea surface without cables. Then, the vehicle will dive to the sea bottom and undertake the predefined near-bottom observation, mapping, and sampling tasks. After the jobs are done, the ARV will automatically drop the ascent ballast and float to the sea surface. The whole operation is carried out through pre-programming with the help of the positioning system and sensors.

Emergency Operation Strategies:

The designers aim to ensure the vehicle's safety, even when some undesired situation happens during sea trials. Therefore, emergency operation strategies and corresponding measures must be designed, programmed, and loaded into the vehicle's control system. Mainly, four scenarios are considered: a break of fiber optic cables, seawater leakage of the control system, malfunction of the computer's main control board, and excessive insulation drop. The vehicle will terminate the operation and float back to the sea surface in these cases.

2.3. Design of the ARV

2.3.1. Main Design Particulars and General Arrangement

A schematic of the ARV model used for the current study is shown in Figure 3, and the main particulars are listed and described as follows:

Main dimensions (length × width × height): 3.2 m × 2.0 m × 1.5 m;
Weight in air: 1.5 tons (including ballast);
Payload: >40 kg;
Operation mode: dual-mode of remote-operated mode and autonomous-operated mode;
System voltage: 128 VDC, 48 VDC, 24 VDC, and 12 VDC;
12 h for the FOD condition with the bottom cruising duration of more than 2 h;
Speed: normal cruising speed of 1.0 knots, maximum speed of 1.5 knots;
Unpowered descending and ascending rate: >40 m/min;

Propulsion: two horizontal thrusters and two vertical thrusters;

Communication: microfiber optic cable, UHF radio;

Positioning and searching: an Iridium satellite beacon, a VHF beacon, an ARGOS beacon, a flasher, a flag, USBL, etc.;

Control: Manual operation, automatic depth, navigation, altitude, hovering.

Most ARVs or AUVs are monohull structures, like ARV Haidou 1. Buoyancy forms are shaped in a streamline and constitute the ARV contour to reduce resistance and improve cruise speed. Also, buoyancy foams can protect main equipment placed inside from unexpected collision during sea trials, but this will also bring in troubles and difficulties with routine equipment maintenance. Therefore, for the design of Dream Chaser, a three-body configuration was adopted, with the main body in the middle and double floating bodies on the left and right sides of the main body. A schematic graph of the ARV is shown in Figure 3. All functional systems are placed on the main body's open-truss frame, and buoyancy foams required for the ARV are completely set in the floating bodies. As a result, routine maintenance will be more convenient for engineers, especially on the sea. Besides, such configuration will be more stable at the sea surface than monohull structures, critical in engineering practice. The general arrangement of facilities and equipment in the main system body is shown in Figure 4.

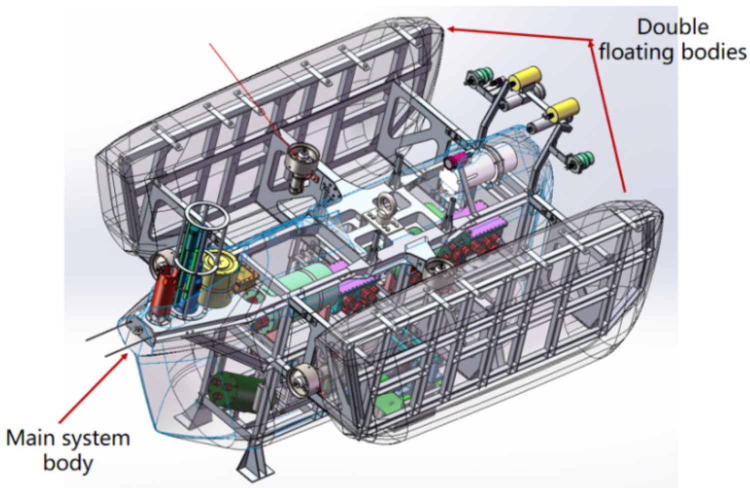

Figure 3. Schematic diagram of the 3D model of the submersible.

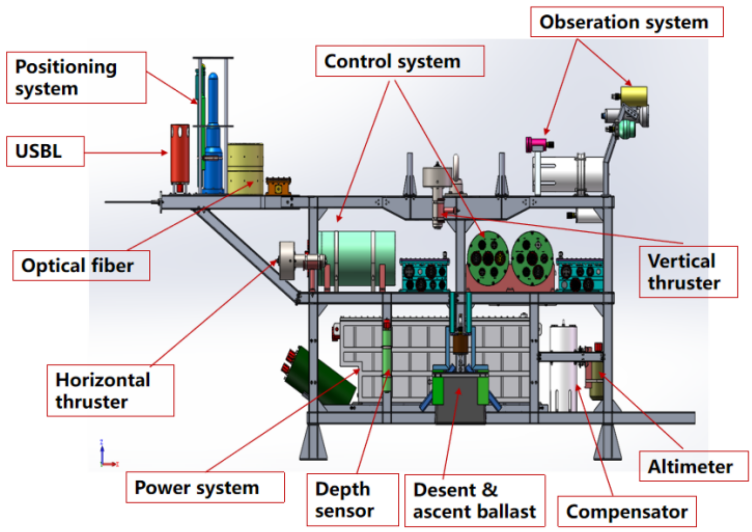

Figure 4. The general arrangement of the main body.

There are three typical hydrostatic analysis conditions: lifting during launching, bottom operating, and recovery. Although the sea trials are commonly carried out from shallow water to 11,000 m step-by-step, the hydrostatic performance in various target depths should be considered for operating conditions. Especially for an FOD ARV, the density of seawater increases significantly from the sea surface to the seabed, bringing more buoyancy. For example, the density of seawater varies and typically increases by 2.8% over a 6000 m depth range [21]. The change will be even bigger over an 11,000 m depth range. On the contrary, the compressibility effects of structures, cables, equipment, etc., will reduce buoyancy when the external pressure increases [22]. Hence, the hydrostatic characteristics of bottom operation conditions for some target depths have been analyzed, as shown in Table 1. It can be found that the ARV has slightly positive buoyancy as designed for each case, and the center of buoyancy is always kept above the center of gravity so that the ARV is self-stable during operation. The origin of the coordinate system was set at the intersection point between the stern section and the central longitudinal section at the keel, with the Z-axis pointing upwards, the X-axis to the ship bow, and the Y-axis to the portside.

Table 1. The hydrostatic parameters for operating conditions of various diving depths.

Submergence Depth	4000 m	6000 m	8000 m	11,000 m
Dry weight (kg)	1362	1375	1385	1403
Displaced volume (m^3)	1,257,591.4	1,258,855.2	1,259,344.4	1,259,994.3
Net buoyancy at bottom (kg)	7.6	7.1	7.5	7.2
Payload (kg)	52	50	45	36
Center of gravity (mm)	(1197,−0.7,710.8)	(1197,−0.7,706.2)	(1197.1,−0.7,697.8)	(1197.1,−0.7,689.4)
Center of buoyancy (mm)	(1182.5,−0.3,798.5)	(1182.5,−0.3,798)	(1182.5,−0.3,797.2)	(1182.5,−0.3,796.2)

In addition, since the equipment of the surface positioning system is located at the stern, the ARV is designed to have a small trim in the bow after floating to the water surface to easily find the vehicle. The freeboard for the top tip of the beacon is 440 mm above the waterline, as shown in Figure 5, which ensures its normal function.

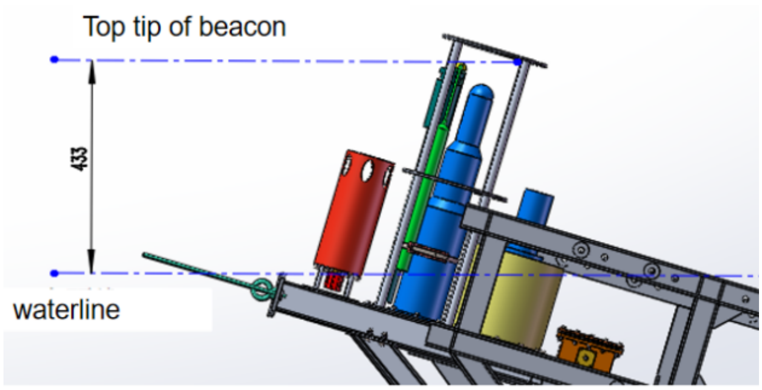

Figure 5. Freeboard of the top tip of the beacon.

The subsystems of the ARV are designed as follows.

2.3.2. Subsystem Design

Buoyancy System Design and Experimental Analysis:

Solid syntactic buoyancy material is used to provide the buoyancy of the submersible. The characteristics of buoyancy material, such as density, compressive strength, minimal crush pressure, water absorption rate, etc., decide the performance of buoyancy material and consequently of the submersible, especially for an FOD submersible. These parameters are interrelated. The damage or loss of buoyancy will bring catastrophic consequences. Considering the importance of buoyancy foams, many water pressure tests for buoyancy foam blocks from various companies have been conducted in the high-pressure chamber of HAST of Shanghai Ocean University. The selection of buoyancy foams largely depends. The high-pressure chamber facility has a maximum test pressure of 180 MPa, and the inner diameter of the chamber is 0.6 m. The pressure tests for simulating the full ocean depth environment with the pressure of 115 Mpa and crushing pressure for various blocks were conducted at a pressurized rate of 0.69–1.72 Mpa/min. A self-developed monitoring system was used to capture the crushing moment. The test equipment and a typical process are shown in Figure 6. The experimental results are shown in Table 2.

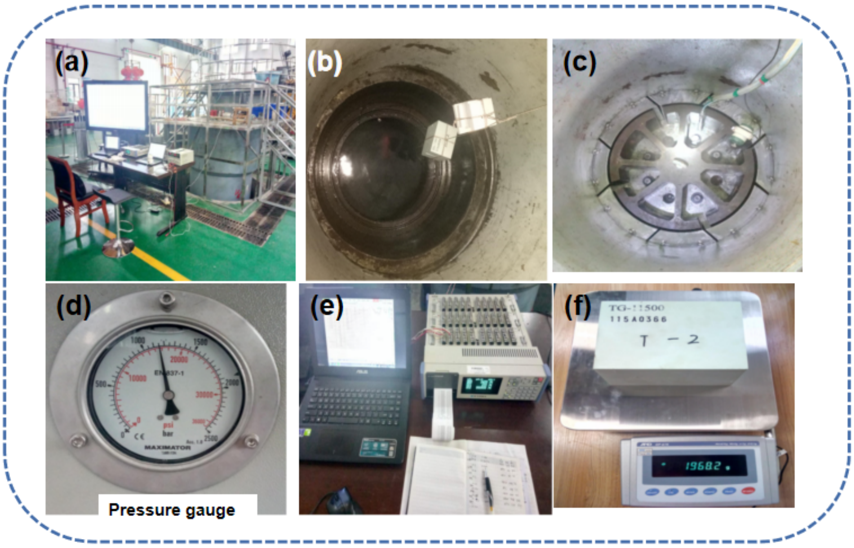

Figure 6. (**a**) The pressure chamber and monitoring system set-up; (**b**) placing buoyancy foam blocks into the chamber; (**c**) closing the chamber cover and getting ready for tests; (**d**) pressure gauge; (**e**) monitoring and data recording during tests; (**f**) weighing the block after the test.

Table 2. Experimental results of buoyancy foam blocks.

Brand	Grade	Block Size/mm	Density (kg/m^3)	Results @Service Pressure	Water Absorption Rate	Hydrostatic Crush (Mpa)
Engineered syntactic systems	HZ-42	610 × 305 × 100	673.0	Intact	<0.1%	>150
Trelleborg	DS-38	609 × 308 × 158	593.0	Intact	<0.1%	>125
Ocean Chemical Research Institute	/	315 × 315 × 100	680.0	Intact	<0.5%	>130

All of the test samples passed the service pressure tests, but they showed different advantages and disadvantages in characteristics. After a comprehensive evaluation, buoyancy foam from Engineered Syntactic Systems of the USA and Ocean Chemical Research Institute of China were used. Product approval tests have also been conducted at service pressure for all blocks. The density and water absorption rate after 115 Mpa pressure test results of 79 HZ-42 blocks are shown in Figure 7, and show steady and consistent performance.

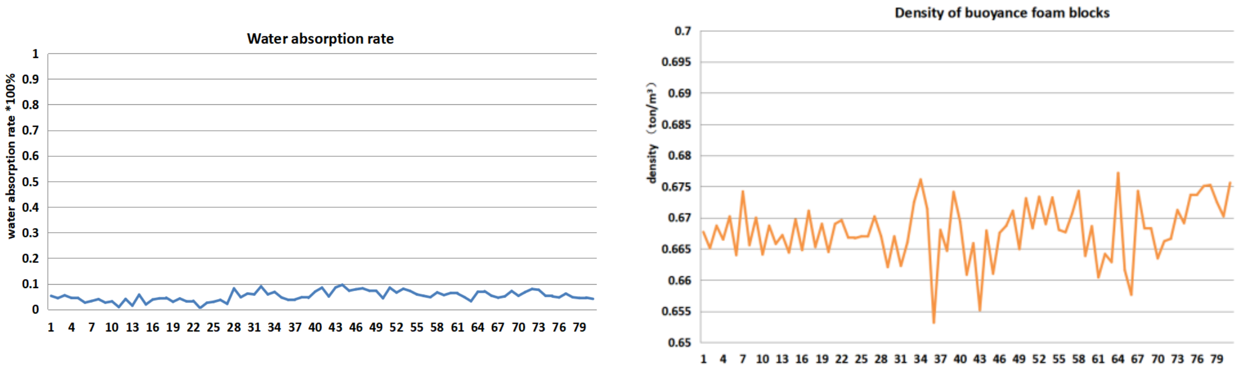

(**a**) (**b**)

Figure 7. (**a**) Water absorption rate; (**b**) density of buoyancy foam blocks.

Structural System Design and Analysis:

The structural system of underwater vehicles typically consists of the frame, pressure-resistant housing, and non-pressure-resistant structures.

The frame structure is used for placing equipment. The aluminum alloy 6061 was used, and a structural strength analysis using finite element method (FEM) was conducted with the software ANSYS for the lifting and fixed conditions according to the rules [23]. The dynamic load factor φ_h is 2.0 and the minimum allowable safety factor is 3.0. The static load was simulated same as the distribution of the equipment on the frame. For the lifting condition, a multi-point constraint (MPC) node was used to simulate the hook point. The von Mises stress, shear stress, and deformations of the frame structure for each condition have been analyzed and proved to satisfy the design requirements. The FEM analysis results is shown in Table 3. The von Mises stress and structural deformation cloud map for the lifting condition are shown in Figure 8. The details of modeling, meshing, and load setting process will not be elaborated here.

Table 3. FEM results for frame structure.

Conditions	Maximum Deformation (mm)	Maximum von Mises Stress (MPa)	Maximum Shear Stress (MPa)	Calculated Safety Factor
Lifting	4.225	78.01	37.11	3.33
Fixed	2.209	59.3	28.84	4.38

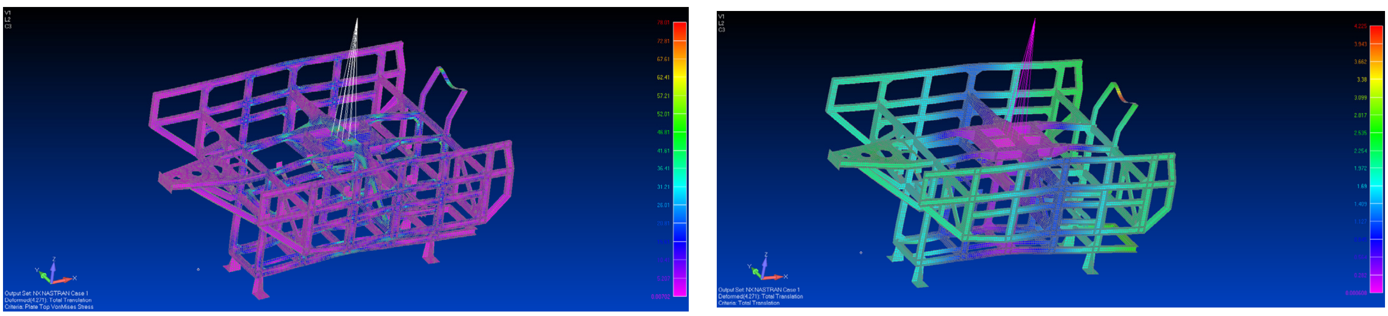

(**a**) (**b**)

Figure 8. (**a**) The von Mises stress cloud map for lifting conditions; (**b**) the structural deformation cloud map for lifting conditions.

The cylindrical hull structure has become a typical marine structure to contain underwater electronic components, which normally cannot work in seawater environments and under huge external pressure. Three pressure chambers are used to contain driving electronics, control system, and video and communication system, respectively, namely PC1, PC2, and PC3. The dimensions and structural scantlings of the PC2 and PC3 are the same. Therefore, the structural analysis for PC1 and PC2 are conducted. The material of titanium alloy TC 4 is used for the pressure hull. An FEM structural strength analysis for all of the pressure hulls has been conducted under external pressure to simulate the full ocean depth environment with a pressure of 115 MPa. External hydrostatic force is set evenly on the shell and heads of the pressure hull in the FEM analysis. Here, since there is no possibility of beyond the maximum design diving depth during ARV operation, the minimum allowable safety factor is lower, down from 1.4 to 1.25, so as to decrease the structural weight of hulls. Likewise, the details of the analysis process are not given here, the FEM results for the pressure hulls are listed in Table 4, and the von Mises stress cloud map of one of the pressure hulls is shown in Figure 9.

Table 4. FEM results for pressure hulls.

Item	Maximum von Mises Stress (MPa)	Positions of the Maximum von Mises Stress	Calculated Safety Factor
Shell of PC1	615	Round fillet at inner shell	1.30
Head of PC1	634	Edge of seal groove	1.26
Shell of PC2	588	Round fillet at inner shell	1.36
Head of PC2	625	Edge of seal groove	1.28

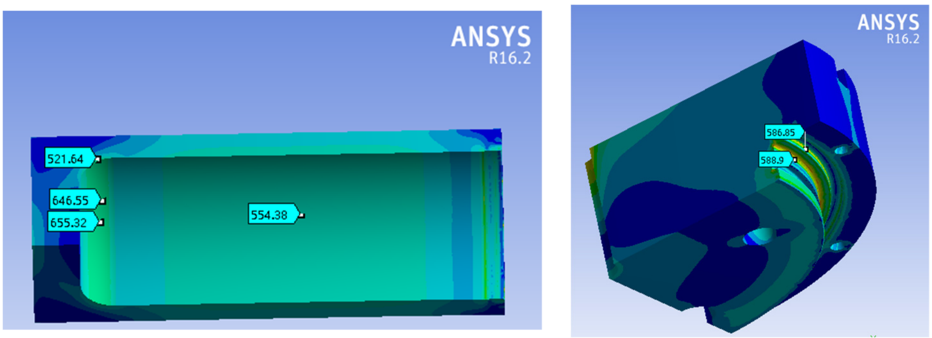

(**a**) (**b**)

Figure 9. (**a**) The von Mises stress cloud map of the hull; (**b**) the von Mises stress cloud map of the cover.

Propulsion System Design and Hydrodynamic Analysis:

The numerical hydrodynamic resistance analysis for designed cruising speed has been conducted using the computational fluid mechanics method. The numerical solution of the governing equations was performed using the commercial computational fluid dynamics code ANSYS Fluent ^{TM} 16.0. The geometric size of the cylindrical computational domain and the boundary conditions imposed for the simulations in this study are shown in Figure 10. The flow inlet is located 1.5L upstream from the fore end of the model, and the flow outlet is located 3.0L downstream from the stern end of the model. Here L is the model length. The cylindrical radius of the computational domain is set as 2.0L after sensitivity tests. The RNG k-ε model is used as the turbulence model. A summary of modeling details is listed in Table 5. The pressure contours in the forward direction and descending direction at a speed v of 1.5 kn and 0.5 kn, respectively, are shown in Figure 11. Due to the length of the paper, the detailed results will not be included in this paper.

The thruster system of the submersible consists of two horizontal thrusters arranged in the stern and two vertical thrusters arranged in the midship of the submersible. The thruster selection is based on the need for maneuverability, resistance to overcome, and reliability issues. The parameters of the thruster are shown in Table 6.

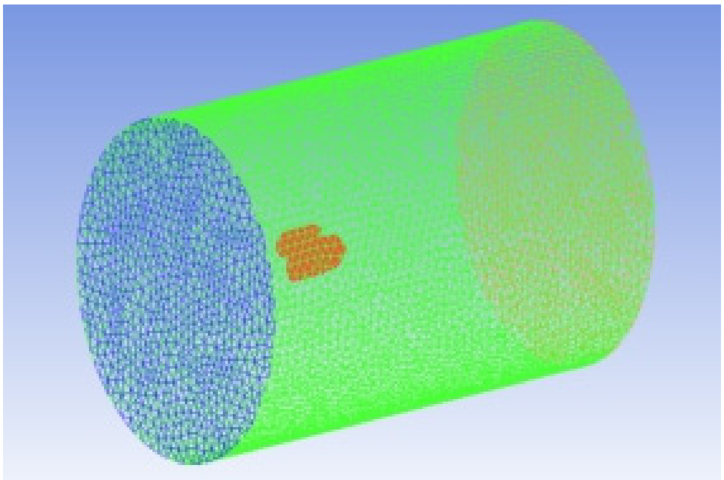

Figure 10. The computational domain.

Table 5. A summary of the numerical analysis settings.

Items	Details
Domain	1.5*L* upstream from the fore end, 3.0*L* downstream from the stern end, 2.0*L* for the radius of the cylindrical domain
Turbulence model	RNG k-ε model non-equilibrium wall function, y+: about 40
P-V coupling	SIMPLE
Momentum	Second-order upwind
Turbulent	Second-order upwind

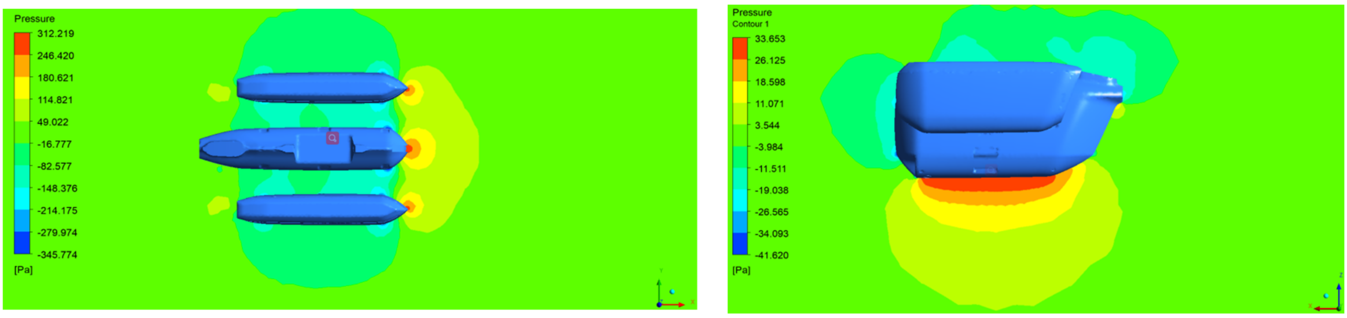

(**a**) (**b**)

Figure 11. (**a**) Pressure contour in the forward direction (v = 1.5 kn); (**b**) pressure contour in the descending direction (v = 0.5 kn).

Table 6. Thruster specification.

Category	Bollard Thrust (kgf)	Voltage (VDC)	Power in (kW)	Nozzle Diameter (mm)	Depth Rating
Horizontal thruster	30 (forward) 30 (reverse)	120	1.5	150	full ocean depth (oil filled)
Vertical thruster	22 (forward) 19 (reverse)	120	1.3	284	full ocean depth (oil filled)

Observation and Communication System Design:

The observation system of the submersible consists of two high-definition cameras arranged in the bow and an ordinary camera to observe the hook between the TMS and submersible body. Also, a backup camera could be set flexibly to watch the motion of the manipulator, the fish cage, or the water sampler. LED lights will be installed together with cameras.

In remotely-controlled mode, the communication between operators and the vehicle connects through fiber optic cables installed in a drum, as shown in Figure 10. The parameters of the fiber optic cable are shown in Table 7. A drum could store up to 25 km of fiberoptic cables. When the ARV returns to the sea surface, the operator could also control the ARV through the UHF radio, as shown in Figure 12, with a maximum range of 10.0 km.

Table 7. The parameters of the fiber optic cable.

Parameter	Outer Diameter (mm)	Weight (g/km)	Attenuation (@1310 nm) (dB/km)	Minimum Bending Radius (mm)	Tensile Strength (N)	Hydrostatic Pressure (MPa)
Value	≤0.45	≤300	≤0.5	≥30	≥90	≥120

(**a**) (**b**)

Figure 12. (**a**) Fiber optic cable drum; (**b**) UHF radio.

Positioning System and Sensors Design:

Multiple types of water surface positioning equipment are chosen for searching, including an Iridium satellite beacon, a VHF beacon, an ARGOS beacon, and a flasher. All of them are shelf products and rated for full ocean depth. In addition, a self-developed ultra-short baseline positioning system (USBL) for full ocean depth is used for underwater positioning. The maximum detection distance of the equipment is 15,133 m, and the real-time positioning accuracy is higher than 0.3% of the slant range, which has been approved through previous sea trials by the authors' team in 2018 [24]. The system composition of the USBL is shown in Figure 13.

Besides, sensors such as altimeters, depth gauges, compass, etc., are also adopted for underwater positioning.

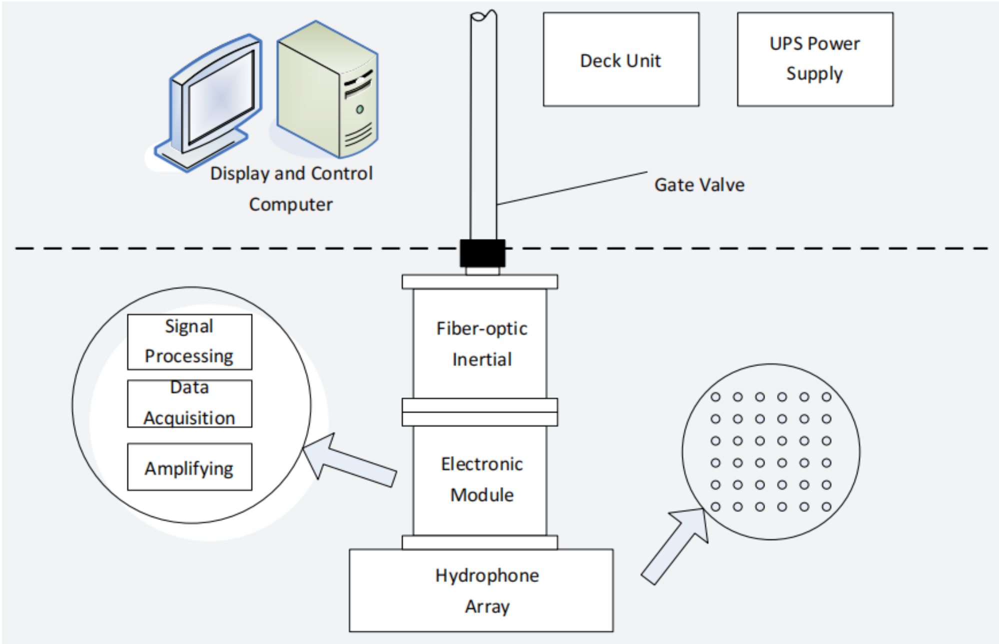

Figure 13. Ultra-short base line positioning system [19].

Electric Power and Power Distribution System Design:

(a) Selection of electric power

The ARV uses its self-installed power energy to perform tasks underwater. According to the operational guidelines for Dream Chaser, the demand for the electricity consumption of each piece of equipment for a typical FOD diving test is counted and summed statistically. Then, the equivalent voltage of each voltage level is converted into 120 VDC, and the obtained power demand for a voltage of 120 VDC is 6683.5 Wh.

After an investigation and initial tests of lead–acid, silver–zinc, and lithium batteries, the lithium battery is adopted in this project. To improve the system's reliability, the battery pack is composed of cells arranged in series connections. According to the analysis of the power demand of the submersible, the capacity of a single cell should be:

$$Q_{cell} = Q_{120v}/120\,\text{V} = 55.70\,\text{Ah} \tag{1}$$

where Q_{120V} is the power demand for voltage of 120 VDC, Q_{cell} is the capacity of a single cell.

The required number of cells for the 120 V battery pack is 33 pieces. However, to ensure that the submersible has a certain amount of power remaining after the operation to complete the surface maintenance and consider the additional electricity demand in emergencies, the final battery pack consists of 40 pieces of 60 Ah batteries. The parameters of the battery are shown in Table 8. To avoid the massive weight of using pressure-resistant housing to contain the cells, pressure-balanced lithium battery technology which is oil-filled is developed with the cells operating at ambient pressure.

(b) Power distribution

For the needs of various electrical equipment, the power is re-distributed and transformed to a series of voltage levels, including 128 VDC for thrusters, 24 VDC for control systems, and another 24 VDC for most of the equipment, and 48 VDC for the manipulator. The power for the control system and equipment power comes from different power modules to isolate the control signal and the terminal equipment. Except for the 128 VDC directly from the battery pack, all other sources are converted through the power module.

Table 8. The battery specifications.

Parameter	Description
Type of battery	Oil-filled lithium battery, with battery management system (BMS)
Capacity	128 VDC, 60 Ah, 40 cells
Working voltage	VDC128V (−10%~+20%), single-cell: 2.5–3.6 V;
Monitor functions	① Capable of temperature, voltage, current, water leakage, and residual power detection; ② Insulation detection.
Environmental requirements	Sea surface: Rolling and pitch ≤ 60°; Underwater: heel ≤ 15° and trim ≤ 30° Operating temperature: 0~50 °C; Storage temperature: 15~40 °C
Service pressure	115 MPa
Maximum pressure	126.5 MPa

Control System Design:

The control system mainly realizes the functions of submersible motion control, operation tool control, sensor data acquisition, status monitoring, fault alarm, real-time video, and other functions. All experimental and monitoring data can be stored locally and remotely, and, at the same time, it provides a man–machine interface for engineers, as shown in Figure 14.

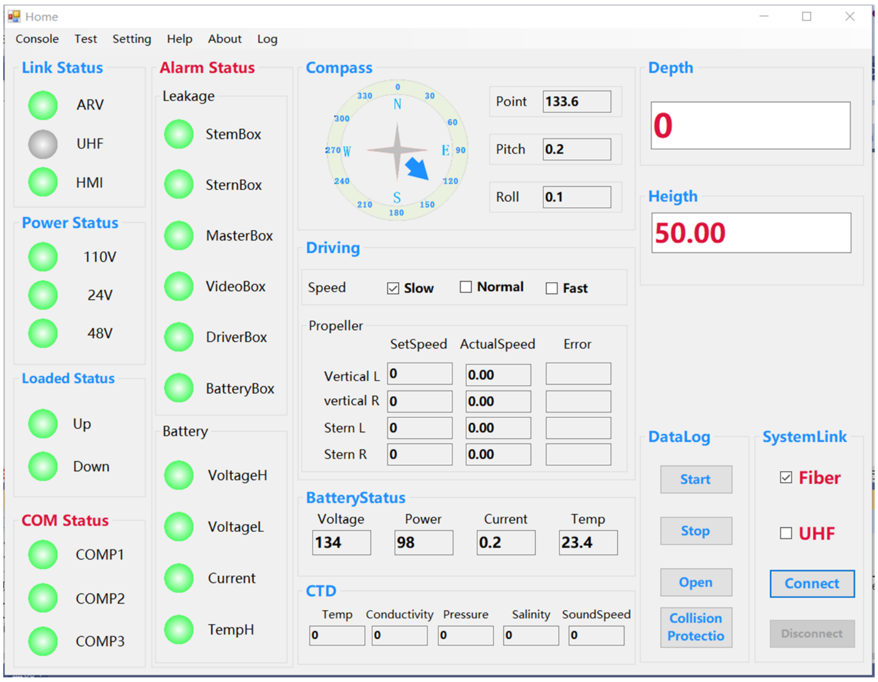

Figure 14. The operation interface of the surface control unit.

The entire control system consists of a surface control unit installed in the integrated control system room and an underwater control system. The surface and underwater are connected by fiber optic cable or UHF. When the ARV is connected through the fiber optic cable, the control signal and video signal can be transmitted in real-time. However, there is only control signal transmission between the surface unit and the vehicle in UHF communication mode, and UHF cannot work underwater. Therefore, this mode is mainly used for submersibles' surface control and deck debugging.

Descent and Ascent Weight and Emergency-Ascent System Design:

Like most deep-sea HOVs, the ARV adopts the philosophy of unpowered descent and ascent strategy with negative buoyancy to descend and positive buoyancy to ascend, which hopes to use less energy during descending and ascending. The change of weight of the vehicle in the water comes from the change of the disposable weight, i.e., descent and ascent weight. A ballast-abandoning mechanism using electromagnets is designed for holding and abandoning the ballast. This ballast also serves as an emergency-ascent ballast, which means throwing the ballast when one of the emergency scenarios is triggered. The descent and ascent weight and the emergency-ascent system are the only mechanisms for emergency safety of the ARV. Therefore, it should be reliable and execute the order correctly every time. Since electromagnets are used, the ballast will drop automatically if the power is off, fails, or runs out. Besides, a delay-abandoning mechanism is set that after a certain period, the ballast will drop as well. A total of three sets of electromagnets are equipped. The design adhesion force of a single electromagnet is 80 kgf.

Tooling System Design:

The tooling system includes a self-developed 11,000 m-rated electric manipulator (shown in Figure 15), macro-biological trapping device, CTD, water sampler, sediments sampler, etc. The ARV is also designed with enough space and interface for future application expansion.

Figure 15. The manipulator installed on the bow of the ARV.

The seven-function electric manipulator is the main operational tool of the ARV, by which most of the sampling operations can be completed. The manipulator can hold more than 25.0 kg at its full extension of 1.0 m. Motors used in industrial manipulators were chosen and then reconstructed to suit the needs of FOD water pressure.

2.4. Design of Other Systems

The TMS, the integrated control system, and the LARS system are very commonly used to operate all kinds of underwater vehicles. However, they are still very important to form up a whole system and successfully apply the underwater vehicles. Since most structures and equipment are quite common, the design of each system is briefly introduced here.

2.4.1. TMS Design

The general arrangement of TMS is shown in Figure 16. The TMS and the submersible body are mechanically connected by hanging and decoupling using an electromagnet mechanism. There are two main functions of the TMS in Dream Chaser. Firstly, it is used to launch the vehicle to a certain depth to avoid surface waves and currents, such that the motions of the vehicle are decoupled from the motions of the support ship. The titanium alloy TC 4 is used for the load-bearing hook. Structural analysis for the hanging condition has been conducted using the software Ansys, as shown in Figure 17. The maximum von Mises stress is 149.34 MPa with a safety factor of 6.2. Secondly, the TMS serves as a communication bridge between the armored electro-optic cable of the ship and fiber optic cables. A pair of drums of electro-optic cables are arranged, with the upper one on the TMS and the lower one on the vehicle, respectively. When the ARV is decoupled from the TMS, the fiber optic cable extracts from both drums as the ARV descends so that the communication keeps connected.

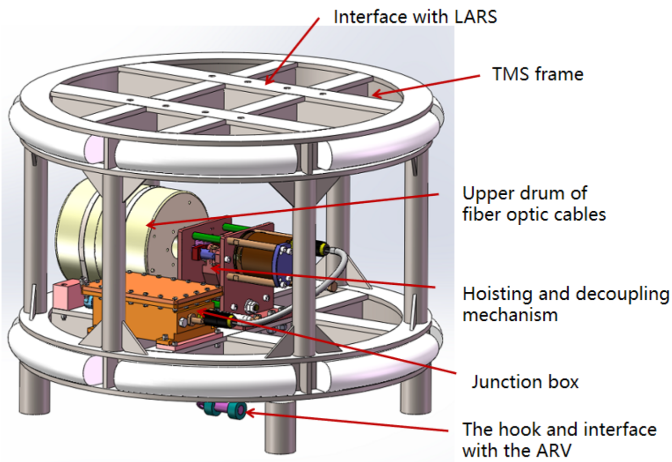

Figure 16. The general arrangement of the TMS.

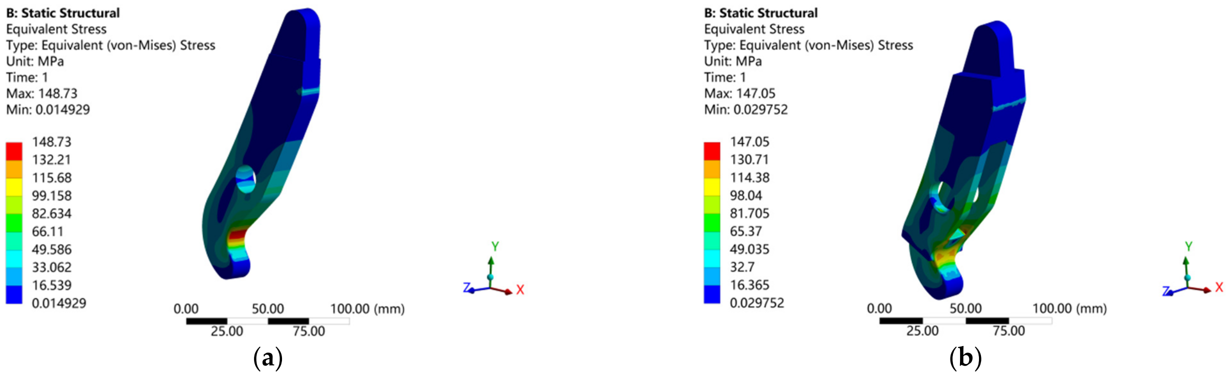

Figure 17. (**a**) Von Mises stress cloud map of the right fork of the hook; (**b**) von Mises stress cloud map of the left fork of the hook.

2.4.2. The Integrated Control System Design

The integrated control system includes an operation console, monitoring equipment, spare parts box, etc. The control system is integrated into a modular container, convenient for transportation. It is fixed on the support ship when working, and the technicians remotely command the submersible through various modules in the container to perform multiple tasks. The container is a standard container with a length of 6 m, a width of 2.43 m, and a height of 2.59 m.

2.4.3. The Launching and Recovery System (LARS) Design

The LARS includes A-frame and skid, winch, electronic-hydraulic power unit, control unit, etc. We use the LARS and the electro-optic cable from the support ship in this project.

3. Laboratory Tests and Results Analysis

3.1. An Overview of the Laboratory Tests

The laboratory tests are a very important phase to validate the function of equipment, find out the systems' problems, and solve them before lake tests or sea trials. On-land functional tests, underwater functional tests, and pressure tests for all components have been conducted. The structural strength and sealing performance of all pressure structures have been carried out with 1.2 times the maximum service pressure. All of the equipment has been tested up to 1.1 times the maximum service pressure in the pressure chamber of HAST. To sum up, 17 structural and mechanical subsystems and a total of 17 subsystems related to electronic systems and equipment have been completed. Lab tests of some key components are described in Section 3.2.

The final assembly and joint debugging tests were carried out on this basis. Like the components tests, the entire system joint debugging tests, including the ARV, the TMS, and the integrated control system, have also been conducted on land, underwater, and in the pressure chamber. All of the functional systems and equipment were put in the pressure chamber, and the whole system could operate correctly in the FOD pressure circumstances for a 12 h duration. The underwater equilibrium and functional tests were then conducted in the water basin of Shanghai Ocean University, as shown in Figure 18. The water basin is 20.0 m in length, 10.0 m in width, and 7.0 m in depth. More than 100 functional tests have been done for both the remotely-operated and autonomously-operated conditions, which show good reliability.

Figure 18. The underwater equilibrium and functional tests in the water basin.

3.2. Key Components Tests and Results Analysis

In this section, lab tests of some of the key components are described.

3.2.1. Descent and Ascent Ballast Mechanism Validation Tests

As mentioned above, the descent and ascent ballast system is key to ensuring safety. The magnetic adhesion capability and the reliability of abandoning weight are the two most important factors that have been tested systematically.

Magnetic Adhesion Tests of the Electromagnets:

The prototype electromagnets were tested both at atmospheric pressure and FOD pressure of 115 MPa, as shown in Figure 19. A consecutive 22 h duration test with hanging weight of 80 kg was conducted. In addition, the adhesion performance of the electromagnets was also undertaken in the pressure chamber. The maximum hydrostatic pressure is 115 MPa with a duration of 14 h at its largest pressure. Three cycles were repeated. There was neither unpredicted ballast-abandoning nor unsuccessful ballast-abandoning throughout each test. The function and reliability of the electromagnet were proved.

(**a**) (**b**)

Figure 19. (**a**) Magnetic adhesion test of the electromagnet; (**b**) magnetic adhesion test in the pressure chamber.

Ballast-Abandoning Performance Test:

The performance of abandoning the ballast under an upright position and inclined 30 and 45 degrees were tested 120 times, and all of the tests were successful in that the ballast dropped smoothly, as shown in Figure 20. In addition, the abandoning test was also conducted in the pressure chamber with a maximum pressure of 140 MPa for 3 h. A total of three repeat tests were carried out, and the ballast was thrown each time smoothly. The function and reliability of the electromagnet and the abandoning mechanism were proved.

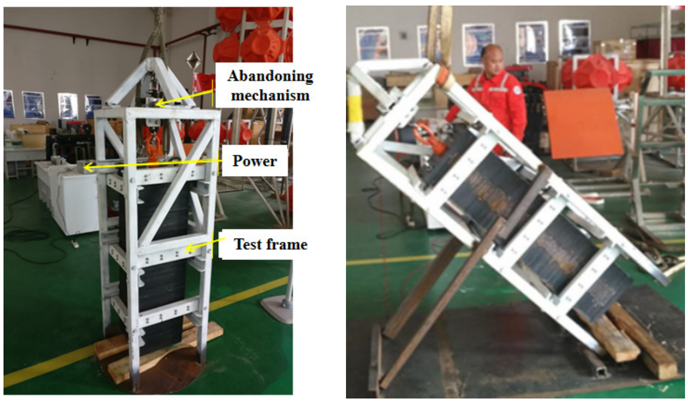

(**a**) (**b**)

Figure 20. (**a**) Ballast abandoning test in the upright position; (**b**) ballast abandoning test in heeling position.

3.2.2. FOD Electric Thruster Tests

Thruster Performance Tests in Various Hydrostatic Pressures:

The open water tests under the hydrostatic pressure of 62 MPa, 115 MPa, and 126 MPa were conducted. Additionally, besides the nominal voltage of 120 VDC, considering the variation range of battery voltage during operation, the performance tests under the voltage of 135 VDC, 120 VDC, and 105 VDC were carried out, respectively, to simulate the decrease of voltage in practical engineering in both the open water tank and pressure chamber. The main conclusions are as follows:

① The pressure test results show that in the voltage range of 105 VDC–135 VDC, the propeller can work well under the service pressure (115 MPa), and the structural integrity is intact under 1.1 times service pressure (126 MPa). Furthermore, the thruster can still work when depressurized to service pressure.

② Regarding bollard thrust performance, the maximum forward thrust is 22 kgf, and the maximum reverse thrust is 19 kgf under the voltage of 120 VDC, which is higher than the requirements.

The Effect of Hydrostatic Pressure on the Efficiency of Thrusters:

Since the output thrust of a propeller under full ocean depth pressure is what we are concerned about, enough efficiency and thrusts should be assured to achieve the design speed. In such circumstances, whether or not the efficiency of a propellor under FOD pressure will be the same as that in the open water basin will be researched here.

Due to the limitation of the size of the pressure chamber, the wake effect of propellers when working can hardly be avoided and neglected. On the other hand, the propeller's thrust in the pressure tests cannot be obtained directly. In such circumstances, the effect of pressure on the thruster's efficiency at a range of FOD is approximately transformed to compare the feedback voltage of thrusters at the same input signal voltage (0–5.0 V) for various hydrostatic pressure since the feedback voltage is proportional to the thrust.

In this section, taking the case of the power voltage of 120 VDC as an example, the input signal voltage and the feedback voltage of the propeller under the open water condition and pressure conditions of 62 MPa and 116 MPa in the pressure chamber have been conducted, respectively. The results are shown in Table 9. Table 9 shows that: (1) As the hydrostatic pressure increases, the propeller efficiency decreases for both forward and reverse conditions. The thrust efficiency at the water pressure of 115 MPa reduces by about 16% compared with that of in the atmospheric pressure in the pressure chamber; (2) compared with the open water condition, the efficiency of the propeller in the pressure chamber is significantly reduced, which is mainly affected by the fluid reflection of the chamber wall.

Table 9. The effect of hydrostatic pressure on the efficiency of thrusters (power voltage; 120 VDC).

Cases		Input Voltage (V)	Feedback Voltage (V)	Efficiency
Open water test (1 atm)	Forward rotation	4.5	3.922	87.16%
Pressure chamber test (1 atm)		4.501	3.72	82.65%
Pressure chamber test (62 MPa)		4.498	3.265	72.59%
Pressure chamber test (116 MPa)		4.502	3.002	66.68%
Open water test (1 atm)	Reverse rotation	−4.505	−4.043	89.74%
Pressure chamber test (1 atm)		−4.508	−4.02	89.17%
Pressure chamber test (62 MPa)		−4.503	−3.836	85.19%
Pressure chamber test (116 MPa)		−4.509	−2.87	63.65%

4. Lake Tests and Results Analysis

After the ARV was assembled, to test the stability and reliability of the system before sea trials, the lake tests were conducted in the Qiandao Lake in Zhejiang province of China from 1 to 6 April 2020, as shown in Figure 21.

The water depth of the site is about 45 m. During tests, the wave and wind were quite small, and obvious bottom currents were found. Instead of using the LARS system, a truss crane was used to launch and recover the ARV. Seven remote-operated mode tests and seven autonomous-operated mode tests were completed. The whole process operation was executed successfully, and all of the main systems and equipment functioned well.

(**a**) (**b**)

Figure 21. (**a**) Launching ARV in Qiandao Lake; (**b**) ARV cruises on the water surface.

5. Sea Trials Results

5.1. South China Sea Trials

From 30 June to 12 July 2020, the first phase sea trial was conducted in the South China Sea with the support ship Xiangyanghong No. 10, as shown in Figure 22. The ship adopts two sets of full rotary rudder propeller electric propulsion system, a dynamic positioning system, and integrated navigation and positioning system. The design displacement is about 4400 tons. The ship has a maximum speed of 12 knots. The LARS system of 'Xiangyanghong No. 10' integrates with a 6000 m armored electro-optic cable and a 6000 m armored steel cable simultaneously, so the launch and recovery of ARV and TMS can use this same A-frame.

Figure 22. A picture of the ship Xiangyanghong No. 10.

The sea trial was divided into five stages: quayside assembly and resuming test, 50 m level sea trials, 200 m level sea trials, 1000 m level sea trials, and 4000 m level sea trials. Nine diving tests were completed in the limited voyage period, with seven remotely-operated mode tests, and one autonomous-operated mode test. The first test was terminated halfway due to an unsuccessful unhook between TMS and the vehicle. The summary of each dive is shown in Table 10. Besides the normal operation tests, emergency tests have been conducted in Dive No. 3, 5, and 6.

The launch process and recovery of the ARV are shown in Figure 23. Through the sea trial, most systems function well and deliver good reliability. The duration of the ARV recovery minimizes from 1 h to 0.5 h as the tests proceed. The near-bottom cruising at the 1000 m level is shown in Figure 24. The placement of the marker and sediment sampling using a self-developed manipulator at Dive No. 8 is shown in Figure 25. During the diving and operation process, the track of the ARV could be traced on board in time through USBL.

After returning from the South China Sea trial test, the project team fully summarized the problems existing in the sea test, completed the technical transformation and upgrading of the first 11,000 m ARV, and developed a backup ARV synchronously.

Table 10. Summary of each dive.

Dive	Location	Date	Depth	Results
1	No record	30 June 2020	9 m	Unsuccessful dive
2	24°41.1 N, 117°06.1 E	2 July 2020	43 m	Remotely-operated mode test
3	21°43.3 N, 116°35.3 E	3 July 2020	180 m	Remotely-operated mode and emergency test
4	20°05.1 N, 115°42.6 E	4 July 2020	1039 m	Remotely-operated mode test
5	20°05.110 N, 115°39.754 E	5 July 2020	1110 m	Remotely-operated mode and emergency test
6	20°05.15 N, 115°39.832 E	6 July 2020	1110 m	Remotely-operated mode and emergency test
7	18°42.0 N, 114°48.0 E	7 July 2020	3575 m	Remotely-operated mode test
8	18°42.005 N, 114°47.992 E	8 July 2020	3577 m	Remotely-operated mode test
9	21°39.9 N, 116°34.2 E	9 July 2020	225 m	Autonomous-operated mode test

(**a**) (**b**)

Figure 23. (**a**) Launching ARV using LARS system; (**b**) ARV on the water surface before disconnection.

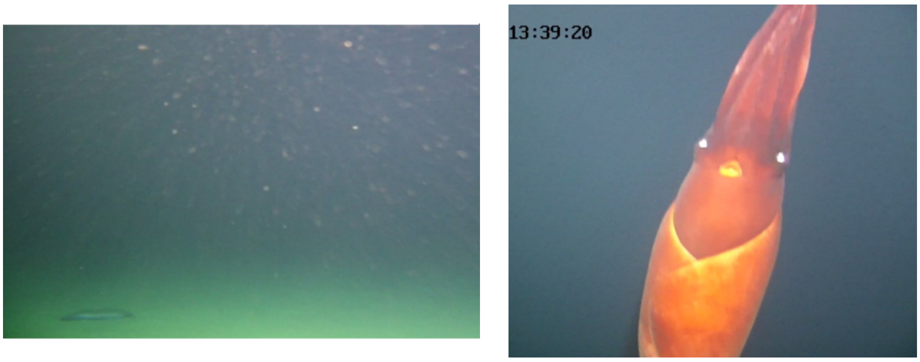

(**a**) (**b**)

Figure 24. (**a**) Near-bottom cruising at 1000 m level; (**b**) deep-sea octopus found in 600 m water depth.

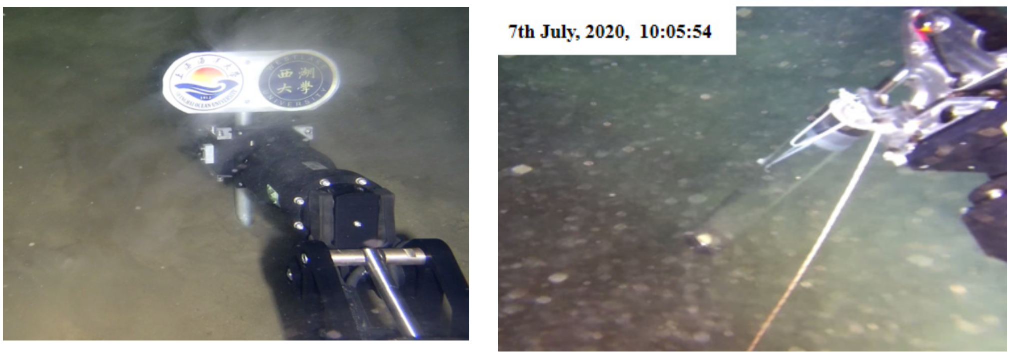

(**a**) (**b**)

Figure 25. (**a**) Placement of the marker at 3577 m water depth; (**b**) sediment sampling.

5.2. Mariana Trench Sea Trials

From 29 November to 30 December 2020, the second phase sea trial was conducted in the South China Sea, the northwest part of the Pacific, and finally in the Mariana Trench with the support ship Shenkuo, as shown in Figure 26. The vessel is a catamaran with a displacement of 2200 tons, and it has a maximum speed of 8 knots. The ship has a dynamic positioning system. The LARS system of 'Shenkuo' integrates with a 6000 m steel cable only. To match the needs of launching and recovery, an 11,000 m electro-optic cable was rented and fixed to A-frame at the quayside.

Figure 26. A picture of the ship Shen Kuo.

The sea trial was divided into six stages: quayside assembly and resuming test, 50 m level sea trials, 1000 m level sea trials, 4000 m level sea trials, 6000 m sea trials, and 11,000 m sea trials. The initial planned duration for the test was 35 days. However, due to the harsh weather, the ship had to take another route which was much longer. Plus, the speed of the ship was much lower than its design. As a result, less than half of the duration was left for the sea trial.

After quayside assembly, resuming test, and shallow water tests, from 11 December to 14 December, the test team conducted three consecutive diving tests, with a maximum diving depth of 6347 m. The entire system of the submersible functioned well, and sediment sampling, water sampling, and other operations were completed. The launch and recovery process is shown in Figure 27. To save time, after the completion of the deep water tests, the mother ship went straight to the Challenger Deep of the Mariana Trench to carry out the 11,000 m sea test. From 19 to 21 December, the team conducted three consecutive trials in the Mariana Trench, with two 6000 m level dives and one 5000 m level dive. Unfortunately, the ARV finally failed to reach the Challenger Deep during tests due to the breakage of fiber optic cables. After the dive on 21 December, the weather forecast showed that there would be even worse sea conditions for the following few days, and the ship's remaining fuel could not afford to hold up to the next environmental window. Furthermore, in the global pandemic situation, fueling was also not possible. In such circumstances, the trial had to be terminated. The summary of each dive is shown in Table 11.

Although the goal set for the Mariana Trench sea trial has not been successfully achieved yet, lessons have been learned and analyzed for the next sea trial.

(1) We should pay more attention to the weak part of a whole system. Sometimes it cannot be fully verified in the laboratory environment, so more emergency plans are needed.

(2) Special attention shall be paid to the impact of swell on the recovery process. During the first dive in the Mariana Trench, it took more than three hours to recover the vehicle after it returned to the sea surface, which is 5–6 times longer than regular recovery. The long recovery made all of the team members exhausted physically and

mentally. Furthermore, many structures were damaged by the collision with the ship. The repair and maintenance also took quite a long time for the next day's trial.

(3) The influence of long operation time for large submergence depth, operation at night, and sudden wind and rain, shall be considered, and emergency plans should be made.

(**a**) (**b**)

Figure 27. (**a**) Launching ARV using LARS system; (**b**) ARV returns to the water surface.

Table 11. Overview of each dive.

Dive	Location	Date	Depth (m)	Results
1	22°32.9′ N, 115°52.1′ E	5 December 2020	22	Remotely-operated mode test
2	21°37.6′ N, 129°55.2′ E	11 December 2020	700	Remotely-operated mode test
3	20°33.4′ N, 131°51.9′ E	12 December 2020	4500	Remotely-operated mode test
4	18°30.3′ N, 132°0.5′ E	14 December 2020	6347	Remotely-operated mode test
5	11°25′ N, 142°30′ E	19 December 2020	5993	Remotely-operated mode test
6	11°25′ N, 142°30′ E	20 December 2020	5924	Remotely-operated mode test
7	11°25′ N, 142°30′ E	21 December 2020	5000	Remotely-operated mode test

6. Summary

This paper proposes and develops a novel three-body 11,000 m rated autonomous and remotely-operated vehicle (ARV) 'Dream Chaser' by the Hadal Science and Technology Center of Shanghai Ocean University. The design of the ARV is comprehensively elaborated, and the design results satisfy the requirements and functions. Components tests, including hydrostatic pressure tests for the pressure of full ocean depth and tank tests, have been completed. Besides, all the equipment and system have been approved to function in the circumstances of FOD pressure in the lab tests. The lake tests and two phases of sea trials have been conducted and analyzed on such a basis. Several large-depth dives have been finished in both remotely-operated and autonomous modes, with the deepest record of 6347 m. All functional equipment has been validated, such as sediment sampling, seawater sampling, and near-bottom cruise. The maintenance and restart of offshore operations can be completed within 24 h. In previous sea trials, the utilization rate of submersible launching operations within the effective time window is more than 90%. The system has high reliability and high economy.

Unfortunately, due to the limited environmental window, the objectives and dream to arrive at the Challenger Deep of Mariana Trench were not achieved during the sea trial in 2020. However, lessons have been learned, such as considering the large scale of swell to the vehicle recovery and potential damage, problems in working at night, fragile components in the whole system and corresponding backup plan, the importance of choosing a support ship, etc. Although the Mariana Trench test failed to achieve the perfect goal due to the short available time window, it also laid a solid technical foundation for the future development and sea trials of the submersible. It will also give guidance for the design of submersibles of this kind.

Author Contributions: Conceptualization and methodology, Z.J., W.C. and J.Z.; methodology, Z.J. and B.W.; software and validation, B.L., J.Z., R.L. and S.Z.; sea trial, Z.J., W.C., B.W., J.Z., R.L., G.L., S.Z. and Z.M.; writing—original draft preparation, Z.J. and B.L.; writing—review and editing, W.C.; project administration, Z.J. and W.C. All authors have read and agreed to the published version of the manuscript.

Funding: This research was funded by the General Program of Natural Science Foundation of Shanghai Committee of Science and Technology 'A multidisciplinary design optimization on the descent and ascent motions of a full ocean depth human occupied vehicle' (Grant No. 19ZR1422700), the scientific innovation program project 'Key technology research, equipment development and application of a 6000 m unmanned submersible with optic detection techniques' by the Shanghai Committee of Science and Technology (Grant No. 20dz1206501) and the Department of Natural Resources of Guangdong Province (Grant No. [2020]027). Also, the engineering project of 11,000 m ARV Dream Chaser was funded by Shanghai Ocean University, Westlake University, and Shutong Hadal Science and Technology Development Foundation, which all the authors also appreciate.

Institutional Review Board Statement: Not applicable.

Informed Consent Statement: Informed consent was obtained from all subjects involved in the study.

Data Availability Statement: The data presented in this study are available on reasonable request from the corresponding author.

Acknowledgments: The efforts of the whole ARV team have been appreciated. The authors are grateful to the crew from the support ships 'Xiangyanghong 10' and 'Shen Kuo' for their help during sea trials.

Conflicts of Interest: The authors declare no conflict of interest.

References

1. UNESCO. *Global Open Oceans and Deep Seabed (GOODS)—Biogeographic Classification*; IOC Technical Series; UNESCO-IOC: Paris, France, 2009; p. 84.
2. Watling, L.; Guinotte, J.; Clarke, M.R.; Smith, C.R. A proposed biogeography of the deep ocean floor. *Prog. Oceanogr.* **2013**, *111*, 91–112. [CrossRef]
3. Jamieson, A. *The Hadal Zone: Life in the Deepest Oceans*, 1st ed.; Cambridge University Press: Cambridge, UK, 2015.
4. Cui, W.C.; Wu, X. A Chinese strategy to construct a comprehensive investigation system for hadal trenches. *Deep Sea Res. Part II Top. Stud. Oceanogr.* **2018**, *155*, 27–33. [CrossRef]
5. Chen, P.; Zhou, H.; Huang, Y.; Xie, Z.; Zhang, M.; Wei, Y.; Li, J.; Ma, Y.; Luo, M.; Ding, W.; et al. Revealing the full biosphere structure and versatile metabolic functions in the deepest ocean sediment of the challenger deep. *Genome Biol.* **2021**, *22*, 207. [CrossRef] [PubMed]
6. Zhang, X.; Xu, Y.; Xiao, W.; Zhao, M.; Wang, Z.; Wang, X.; Xu, L.; Luo, M.; Li, X.; Fang, J.; et al. The hadal zone is an important and heterogeneous sink of black carbon in the ocean. *Commun. Earth Environ.* **2022**, *3*, 25. [CrossRef]
7. Kohnen, W. Human exploration of the deep seas: 50 years and the inspiration continues. *Mar. Technol. Soc. J.* **2009**, *43*, 42–62. [CrossRef]
8. Fryer, P.; Becker, N.; Appelgate, B.; Martinez, F.; Edwards, M.; Fryer, G. Why is the Challenger Deep so deep. *Earth Planet. Sci. Lett.* **2003**, *211*, 259–269. [CrossRef]
9. Than, K. James Cameron Completes Record-Breaking Mariana Trench Dive. Available online: https://www.nationalgeographic.com/adventure/article/120325-james-cameron-mariana-trench-challenger-deepest-returns-science-sub (accessed on 25 March 2012).
10. Greenaway, S.F.; Sullivan, K.D.; Umfress, S.H.; Beittel, A.B.; Wagner, K.D. Revised depth of the Challenger Deep from submersible transects; including a general method for precise, pressure-derived depths in the ocean. *Deep Sea Res. Part I Oceanogr. Res. Pap.* **2021**, *178*, 103644. [CrossRef]
11. Du, M.; Peng, X.; Zhang, H.; Ye, C.; Dasgupta, S.; Li, J.; Li, J.; Liu, S.; Xu, H.; Chen, C.; et al. Geology, environment, and life in the deepest part of the world's oceans. *Innovation* **2021**, *2*, 100109. [CrossRef]
12. Fletcher, B.; Bowen, A.; Yoerger, D.R.; Whitcomb, L.L. Journey to the Challenger Deep: 50 Years Later with the Nereus Hybrid Remotely Operated Vehicle. *Mar. Technol. Soc. J.* **2009**, *43*, 65–76. [CrossRef]
13. Takagawa, S. Advanced technology used in Shinkai 6500 and full ocean depth ROV Kaiko. *Mar. Technol. Soc. J.* **1995**, *29*, 15–25.
14. Momma, H.; Watanbe, M.; Hashimoto, K.; Tashiro, S. Loss of the full ocean depth ROV Kaiko, part 1: ROV Kaiko, A review. In Proceedings of the 14th International Offshore and Polar Engineering Conference, Toulon, France, 23–28 May 2004.
15. Yoshida, H.; Ishibashi, S.; Watanabe, Y.; Inoue, T.; Tahara, J.; Sawa, T.; Osawa, H. The ABISMO Mud and Water Sampling ROV for Surveys at 11,000 m Depth. *Mar. Technol. Soc. J.* **2009**, *43*, 87–96. [CrossRef]

16. Kostel, K. Kermadec Trench Expedition 2014: A Sad Day. Available online: http://web.whoi.edu/hades/a-sad-day/ (accessed on 10 May 2014).
17. Jia, L. Chinese Unmanned Submersibles Descend 10,000 Meters Underwater. Available online: http://english.cas.cn/newsroom/china_research/201612/t20161230_173047.shtml (accessed on 30 December 2016).
18. Wikipedia. Vityaz-D Autonomous Underwater Vehicle. Available online: http://en.volupedia.org/wiki/Vityaz-D_Autonomous_Underwater_Vehicle (accessed on 27 May 2022).
19. Xinhua. 10,907 Meters Under Sea! China's Unmanned Submersible Sets New Record. Available online: http://www.chinadaily.com.cn/a/202006/09/WS5edf1df4a310834817251d07.html (accessed on 9 June 2020).
20. Cui, W.C.; Hu, Y.; Guo, W.; Pan, B.B.; Wang, F. A preliminary design of a movable laboratory for hadal trenches. *Methods Oceanogr.* **2014**, *9*, 1–16. [CrossRef]
21. McPhail, S. Autosub6000: A Deep Diving Long Range AUV. *J. Bionic Eng.* **2009**, *6*, 55–62. [CrossRef]
22. Jiang, Y.Q. Statics variation analysis due to spatially moving of a full ocean depth autonomous underwater vehicle. *Int. J. Nav. Archit. Ocean Eng.* **2019**, *11*, 448–461. [CrossRef]
23. China Classification Society. *Rules for Construction and Classification of Diving Systems and Submersibles*; China Communications Press: Beijing, China, 2013.
24. Cui, W.C.; Zhou, X.; Jiang, Z. Ultra-Short Baseline Positioning System for Full Ocean Depth. *Eng. Technol.* **2019**, *3*, 555601.